

Simulation of Channel Electron Mobility Due to Scattering with Interfacial Phonon-Plasmon Modes in Silicon Nanowire under the Presence of High-k Oxide and Metal Gate

Kai Xiu

IBM Semiconductor Research and Development Center (SRDC), 2070 Route 52, Hopewell Junction, NY 12533
Email: kaixiu@us.ibm.com

Abstract—The channel electron mobility of a 1D nanowire due to scattering with interfacial phonon-plasmon modes arising from the high-k dielectric material under the presence of polysilicon or metal gate is studied in this manuscript. We solved the dispersion relationship of the coupled modes and the accompanying effective scattering potential for carrier relaxation in the channel. The resulting mobility was calculated for a series of geometrical configurations with polysilicon/metal as the gate material. We found that for the polysilicon gate case the mechanism gives rise to a significantly low mobility in the low to mid electrical field range, and that wires with smaller diameter suffer more heavily. Our simulation also reveals that metal gate effectively mitigates the effect through the suppression of effective scattering field.

Keywords – silicon nanowire, mobility, high-k, silicon, metal gate, soft phonon, plasmon, dielectrics, dynamic screening, HKMG

I. INTRODUCTION

Silicon nanowires are promising candidates for next generation MOSFET devices in the post-Moore's-law era due to their favorable short channel effect and excellent carrier transport characteristics [1]. Replacing the gate dielectric SiO_2 with a high-k material and using a metal gate electrode (HKMG) for the nanowire can potentially further improve its electrostatics. Historically, extensive experimental and theoretical works have been performed on 2D planar MOSFET devices with regards to the impact of soft polar phonons in high-k dielectrics on mobility degradation, though there is still a lack of understanding in literature on its 1D counterpart. It is thus the purpose of this manuscript to theoretically study the same phenomenon as it is applied to the 1D geometry. Specifically, we focus our attention on the determination of coupled interfacial phonon-plasmon modes and the carrier relaxation under its presence. Our theoretic treatment follows closely of Refs. [2] and [3], which dealt with the soft-phonon scattering in a 2D planar MOSFET device, and it reveals distinctive features which are associated with the unique 1D geometry of the nanowire.

As depicted in Fig. 1, the structure of interest features a simplified, ideal circular-shaped cylinder of silicon with high-k gate oxide and gate contact being wrapped around in turn. The structure guarantees a well defined wave vector along the longitudinal direction. A few assumptions are taken throughout this paper for the sake of clarity: the polysilicon gate is treated

as a static dielectric material with its dielectric coefficient being $\epsilon_{\text{GATE}} = \epsilon_{\text{Si}}^0 = 11.7$ independent of the frequency; the phonon spectrum of high-k material is assumed to be that of HfO_2 , with only its lower TO mode being considered, namely, we have

$$\epsilon_{hk}(\omega) = \epsilon_{hk}^{\infty} + (\epsilon_{hk}^0 - \epsilon_{hk}^{\infty}) \frac{\omega_{TO}^2}{\omega_{TO}^2 - \omega^2} \quad (1)$$

with $\epsilon_{hk}^{\infty} = 5.03$, $\epsilon_{hk}^0 = 22$ and $\omega_{TO} = 12$ meV; As for the dielectric property of the metal gate we follow the same practice as in Ref. [4] in which it is treated as an ideal non-penetrating region so that $\epsilon = 0$.

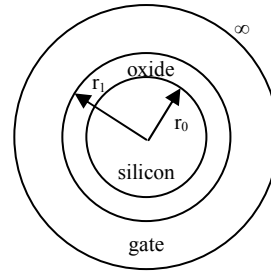


Fig. 1. Circular cross section of an uniaxial silicon nanowire. The device structure being considered is simplified as three layers of materials: body silicon as the inner most; gate oxide as the second and gate electrode as the outer layer.

II. THEORETICAL CONSIDERATION

A. Determination of Eigensystem and Interfacial Phonon-Plasmon Coupled Mode

We start with the procedure of obtaining eigenstates of the 1D system as shown in Fig. 1. It consists of a self-consistent solution of the Schrodinger and Poisson equations in the domain for various gate voltages. By assuming a perfect angular symmetry we can express the in-plane component of the single-particle as $\phi_{\mu}(r) = \frac{1}{\sqrt{2\pi}} \kappa_{\mu}(r) e^{im\theta}$, where $\kappa_{\mu}(r)$ is the solution of Schrodinger equation in radial coordinate

$$\left[-\frac{\hbar^2}{2m} \frac{1}{r} \frac{\partial}{\partial r} \left(r \frac{\partial}{\partial r} \right) + V_{\text{eff}}(r) \right] \kappa_{\mu}(r) = E_{\mu} \kappa_{\mu}(r) \quad (2)$$

Here $V_{\text{eff}}(r)$ is electrostatic potential determined by the accompanying Poisson equation.

Dynamic screening of the optical phonon field arising from the existence of high-k dielectric materials and its impact on mobility degradation are the focuses of our discussion in this section. This phenomenon is also commonly termed as phonon-plasmon coupled mode, and it represents the collective optical phonon excitation under the influence of dynamic response of the high density mobile carriers in the channel. Consequently, the corresponding dispersion relationship shares the nature of native ones of each individual region (i.e. polar optical phonons in high-k gate dielectrics and plasmons in the silicon channel inversion layer in our discussion), and as what will be discussed in the following, is a direct solution of the interface continuity requirements for electric field and displacement.

For a non-vanishing longitudinal electric field, the specific (transverse magnetic) solution to the Maxwell equation that describes the electromagnetic propagation must ensure that the longitudinal electric field is continuous across the oxide-silicon interface. By ignoring retardation effects and assuming an ideal cylindrical symmetry for the domain being considered, we can decompose the associated electrostatic potential $\varphi_\omega(r, z) = \frac{1}{L} \sum_q \varphi_{\omega q}(r) e^{iqz}$ where q is the wave vector of the traveling wave. The q -component potential $\varphi_{\omega q}(r)$ satisfies the Laplace equation in radial coordinate

$$\left(\frac{\partial^2}{\partial r^2} + \frac{1}{r} \frac{\partial}{\partial r} - q^2 \right) \varphi_{\omega q}(r) = 0 \quad (3)$$

and its general solution can be written as

$$\varphi_{\omega q}(r) = \begin{cases} a(q, \omega) I_0(qr) & 0 < r < r_0 \\ b(q, \omega) I_0(qr) + c(q, \omega) K_0(qr) & r_0 < r < r_1 \\ d(q, \omega) K_0(qr) & r > r_1 \end{cases} \quad (4)$$

Here $I_n(x)$ and $K_n(x)$ are the n -th order modified Bessel function of the first and second kind. To solve the unknown coefficients $a(q, \omega)$, $b(q, \omega)$, $c(q, \omega)$, and $d(q, \omega)$ we apply the requirement of continuity of longitudinal component of the electric field and radial component of the electric displacement cross each interface. The latter can be written in a generalized form as

$$D(q, \omega, r) = -\frac{\partial \varphi_{\omega q}^{all}(r)}{\partial r} = -\int_0^\infty \varepsilon(q, \omega, r, r') \frac{\partial \varphi_{\omega q}^{all}(r')}{\partial r'} r' dr' \quad (5)$$

Here $\varphi_{\omega q}^{all}(r)$ is the self-consistent total potential in response to $\varphi_{\omega q}(r)$. It should also be noted that the non-local feature of permittivity in (5) persists only in the channel silicon region. We are thus able to write explicitly the interface boundary condition for the two interfaces as

$$\begin{aligned} \int_0^\infty \varepsilon(q, \omega, r, r') \frac{\partial \varphi_{\omega q}(r')}{\partial r'} r' dr' \Big|_{r=r_0}^- &= \varepsilon_{hk}(\omega) \frac{\partial \varphi_{\omega q}(r)}{\partial r} \Big|_{r=r_0}^+ \\ \varepsilon_{hk}(\omega) \frac{\partial \varphi_{\omega q}(r)}{\partial r} \Big|_{r=r_1}^- &= \varepsilon_{gate}(\omega) \frac{\partial \varphi_{\omega q}(r)}{\partial r} \Big|_{r=r_1}^+ \\ \varphi_{\omega q}(r) \Big|_{r=r_0}^- &= \varphi_{\omega q}(r) \Big|_{r=r_0}^+ \\ \varphi_{\omega q}(r) \Big|_{r=r_1}^- &= \varphi_{\omega q}(r) \Big|_{r=r_1}^+ \end{aligned} \quad (6)$$

Combining these conditions we can determine three unknowns of $b(q, \omega)$, $c(q, \omega)$, and $d(q, \omega)$ and leave the last unknown magnitude coefficient $a(q, \omega)$ to be discussed in the next section.

We are now interested in determining the form of the non-local dielectric tensor $\varepsilon(q, \omega, r, r')$ appearing in boundary conditions (6). This term represents the exclusive plasmon response to external electrostatic fields of inversion electrons under a 1D cylinder geometry. Keeping in mind that $\varphi_{\omega q}(r)$ is the applied external potential as the solution of Eqn. (3) and $\varphi_{\omega q}^{all}(r)$ is its self-consistent total response, we can relate these two properties by

$$\varphi_{\omega q}^{all}(q, \omega, r) = \varphi(q, \omega, r) + \frac{1}{\varepsilon_\infty} \int_0^{r_0} r' G_q(r, r') \delta \rho_{q\omega}(r') dr' \quad (7)$$

with the help of the Green function. The Green function and induced charge density $\delta \rho_{q\omega}(r')$ take the forms [4]

$$\begin{aligned} G_q(r, r') &= I_0(qr) K_0(qr') \\ \delta \rho_{q\omega}(r') &= \frac{e^2}{2\pi} \sum_{mn} \Pi_{mn}(q, \omega) \varphi_{mn}^{all}(r') \kappa_m(r) \kappa_n(r) \\ \varphi_{mn}^{all} &= \int_0^{r_0} \varphi_{mn}^{all}(q, \omega, r) \kappa_m(r) \kappa_n(r) r dr \end{aligned} \quad (8)$$

Here we denote $\Pi_{mn}(q, \omega)$ as the standard 1D RPA polarization function [5]

$$\Pi_{mn}(q, \omega) = \frac{2}{L} \sum_k \frac{f(E_m(k)) - f(E_n(k+q))}{E_m(k) - E_n(k+q) + \hbar\omega + i0^+} \quad (9)$$

Using these notations, we can now explicitly write the electric displacement as

$$D_r(q, \omega, r) = -\varepsilon_\infty \frac{\partial \varphi_{\omega q}(r)}{\partial r} - \frac{\partial}{\partial r} \int_0^{r_0} r' G_q(r, r') \delta \rho_{q\omega}(r') dr \quad (10)$$

A combination of Eqns. (5), (7) and (10) shall be solved numerically. In practice, we have found that by applying the Hartree approximation which replaces $\varphi_{\omega q}^{all}(r)$ with $\varphi_{\omega q}(r)$ in the expression of $\varphi_{mn}^{all}(r)$ in (8), we can effectively reach an explicit formula of the dielectric coefficient

$$\varepsilon(q, \omega, r, r') = \varepsilon_{Si}^\infty \left(1 - \frac{e^2 K_1(qr)}{2\pi \varepsilon_{Si}^\infty I_1(qr')} \sum_{mn} \Pi_{mn}(q, \omega) |\varphi_{mn}^{all}|^2 \right) \quad (11)$$

and use it without losing too much accuracy.

The solution of effective dielectric coefficient (11) enables us to obtain the dispersion relationship of interfacial phonon-plasmon mode by solving the secular equations (6). Typical numerical solutions under certain gate biases, which take the form $\omega(q) = \omega_q$, are shown in Figs. 2 and 3. In Fig. 2, we plot both the pure plasmon dispersion curve (obtained by letting the high-k dielectrics respond with static ε_{hk}^0) and the coupled ones. The impact of plasmon response to the coupled mode is evident in the long-wave range. It should be noted that there are two coupled branches for one bulk TA phonon mode. This is the consequence of the symmetry associated with the 1D

structure and it can be easily shown that the lower branch has a negligible scattering strength so it will be dismissed in our calculation. The impact of metal gate is best illustrated in Fig. 3, where we plot the upper branch of the coupled mode for three scenarios: static optical phonon only (obtained by letting the channel respond with static ϵ_{Si}^0); coupled with polysilicon gate and coupled with metal gate. It can be seen that by replacing the polysilicon gate with the metal one provides a strong attenuation over the dispersion energy through the image effect. This effect is especially prominent in the smaller diameter case and higher charge concentration range.

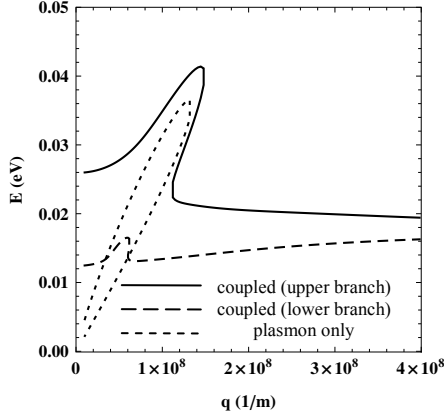


Fig. 2. Dispersion relationships between the polar phonon induced electromagnetic excitations and wave factor for phonon-plasmon modes (solid and dashed lines) and plasmon mode only (dotted line) in a silicon nanowire with $r_0=6$ nm and $r_1=10$ nm. The inversion charge density is 8×10^8 1/m.

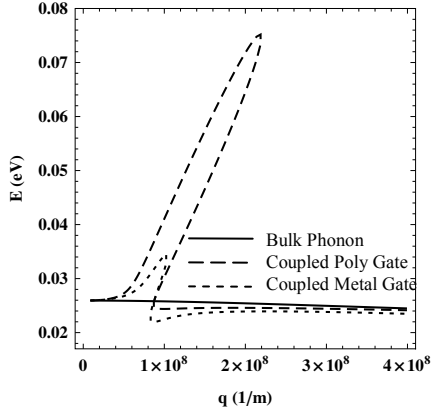


Fig. 3. Dispersion relationships (upper branches) between the polar phonon induced electromagnetic excitation modes and wave factor for various scenarios of interfacial coupling in a silicon nanowire. The solid curve represents the “pure” bulk polar phonon mode, and the dotted (metal gate) and dashed (polysilicon gate) curves are coupled modes in which the coupling with the channel electron induced plasmon mode is taken into consideration. The impact of the metal gate is visible in that it provides a strong attenuation over the mode potential through the image effect.

B. Determination of Effective Potential

In the previous subsection we obtained coefficients $b(q, \omega)$, $c(q, \omega)$, and $d(q, \omega)$ associated with the electrostatic potential (4) with only the channel amplitude $a(q, \omega)$ left undetermined. A semiclassical approach is adopted, whose details can be found Ref. [3], in which we equalize the time averaged total

electrostatic energy associated with the optical phonon field to the zero-point energy of a harmonic oscillator,

$$\langle W(q, t) \rangle = 2 \int_0^{\infty} \rho_q(r) \varphi_q(r) r dr = \frac{1}{2} \hbar \omega \quad (12)$$

with $\rho_q(r)$ being the sum of net charges existing at each interface

$$\begin{aligned} \rho_q(r) = & I_{00} [a(q, \omega) \epsilon_{CH}(q, \omega) I_{10} - b(q, \omega) \epsilon_{OX}(\omega) I_{10} \\ & + c(q, \omega) \epsilon_{OX}(\omega) K_{10}] \delta(r - r_0) + K_{01} [b(q, \omega) \epsilon_{OX}(\omega) I_{11} \\ & - c(q, \omega) \epsilon_{OX}(\omega) K_{11} + d(q, \omega) \epsilon_{GATE}(q, \omega) K_{11}] \delta(r - r_1) \end{aligned} \quad (13)$$

with $I_{ij} = I_i(qr_j)$ and $K_{ij} = K_i(qr_j)$

Consequently we have

$$a(q, \omega) = \left(\frac{\hbar \omega}{4\pi_0 q \epsilon_{TOT}(q, \omega)} \right)^{1/2} \quad (14)$$

Here the lumped property $\epsilon_{TOT}(q, \omega)$ is viewed as the total effective dielectric function of the coupled system

$$\begin{aligned} \epsilon_{TOT}(q, \omega) = & I_{00} [\epsilon_{CH}(q, \omega) I_{10} - b(q, \omega) \epsilon_{OX}(\omega) I_{10} \\ & + c(q, \omega) \epsilon_{OX}(\omega) K_{10}] + d(q, \omega) K_{01} [b(q, \omega) \epsilon_{OX}(\omega) I_{11} \\ & - c(q, \omega) \epsilon_{OX}(\omega) K_{11} + d(q, \omega) \epsilon_{GATE}(q, \omega) K_{11}] r_1 / r_0 \end{aligned} \quad (15)$$

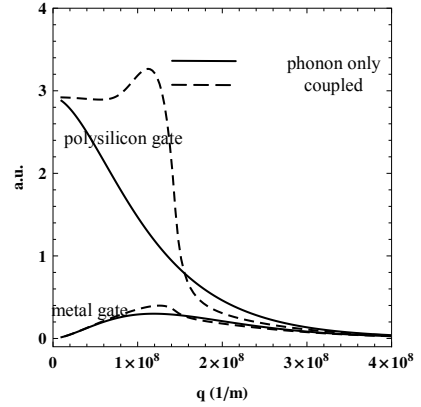


Fig. 4. Effective potential (value at the silicon/oxide interface) as a function of wave vector. Solid lines are phonon-only contributions without plasmon coupling and dashed lines are coupled-mode contributions. The upper set of data corresponds to the polysilicon gate and the lower set the metal gate.

As indicated in Ref. [3] the amplitude $a(q, \omega)$, or equivalently the total dielectric function $\epsilon_{TOT}(q, \omega)$ containing the channel plasmon contribution $\epsilon_{CH}(q, \omega)$ as well as the polar phonon contribution $\epsilon_{OX}(q, \omega)$, is a place holder whose root is identical to the exact coupled-mode dispersion relationship if we equalize $\epsilon_{CH}(\omega) = \epsilon(q, \omega)$ in (11) and $\epsilon_{OX}(\omega) = \epsilon_{hk}(\omega)$ in (1). To account for the selective individual TA phonon contribution, one needs to take the difference between the square of amplitude of the two $a(q, \omega)$'s with one $\epsilon_{TOT}(q, \omega)$ representing the full phonon-plasmon response as we indicated above and the other one $\epsilon_{TOT}^0(q, \omega)$ being the response of the “frozen” phonon, namely, $\epsilon_{TOT}^0(q, \omega) = \epsilon_{TOT}(q, \omega) \Big|_{\epsilon_{OX} = \epsilon_{hk}^0}$. The final form for the effective field is thus given by

$$|\phi_q(r)|^2 = \frac{\hbar\omega}{4\pi_0q} \left(\frac{1}{\varepsilon_{TOR}(q, \omega)} - \frac{1}{\varepsilon_{TOR}^0(q, \omega)} \right) |I_0(qr)|^2 \quad (16)$$

In Fig. 4 we plot a typical case of effective field value at silicon-oxide interface. A notable feature is the influence of the plasmon impact denoted by dashed lines. Such interaction increases the field strength in the low- q (long wave) range and decreases below the pure phonon strength in the mid to high- q range. It is also shown that the field strength is suppressed significantly under the presence of metal gate.

III. MOBILITY CALCULATION AND DISCUSSION

Using the Fermi golden rule, we can express the momentum relaxation time due to the emission and absorption of a coupled interfacial phonon-plasmon mode of a certain subband μ as

$$\frac{1}{\tau_\mu(k)} = \frac{e^2}{\varepsilon_0\hbar} \sqrt{\frac{2m}{\hbar^2}} \frac{1}{\sqrt{E + \hbar\omega - E_\mu}} \sum_q |v_\mu(q)|^2 \left\{ \begin{matrix} n_q \\ n_q + 1 \end{matrix} \right\} \times \quad (17)$$

$$\times \frac{1 - f(E \pm \hbar\omega)}{1 - f(E)} \left(\frac{1}{\varepsilon_{TOR}(q)} - \frac{1}{\varepsilon_{TOR}^0(q)} \right) \theta(E + \hbar\omega - E_\mu)$$

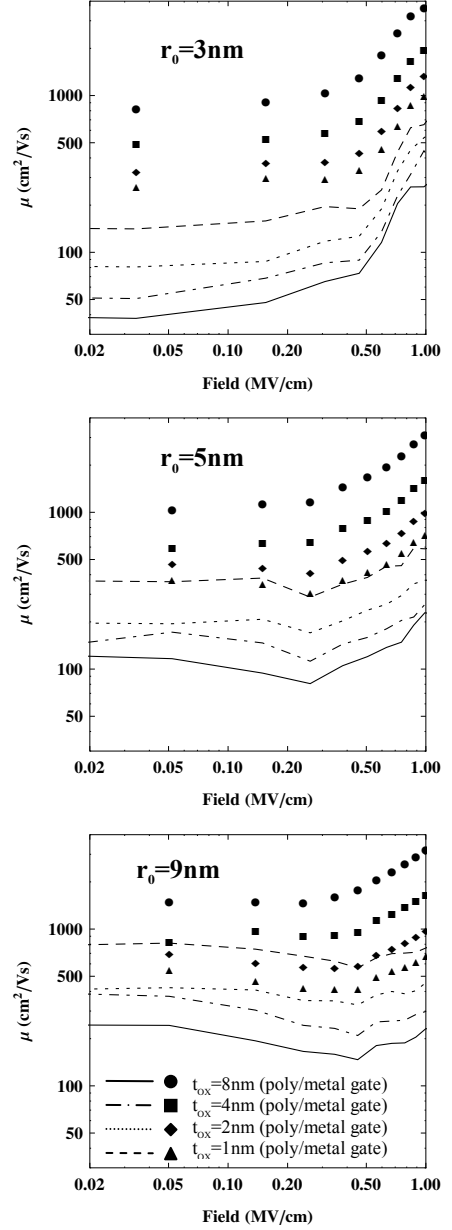
where n_q and $f(E)$ are the Bose and Fermi distributions and $v_\mu(q) = \int_0^{r_0} r \kappa_\mu^2(r) I_0(qr) dr$. The ensuing mobility as a function of interface electrical field strength is shown in Figs 5, 6 and 7. In each figure we showed a specific body silicon radius with four set of data corresponding to different HfO₂ thicknesses. Also in each plot the distinctions between the polysilicon gate and metal gate are drawn. The trend of mobilities indicates that electron scattering with interfacial plasmon-phonon is less severe at high field region, where strong inversion can better screen the polar phonon field. This is especially manifested in the small diameter case. Smaller diameter cases also display a more significant mitigating effect from the introduction of metal gate (Fig. 5).

Before concluding our discussion for mobility calculation we stress the fact that the effective field strength in (16) is “phonon-like” by its definition although we did not apply the notion of phonon content ratio that was used in Ref [3]. This could have a potential problem of overestimating the mobility degradation in the high field range. However, this practice is partly justified by noticing the fact that while plasmon content impacts much in the low- q region as indicated by Fig. 4, it usually involves with the exchange of much higher energy given the nature of the dispersion relationship as shown in Fig. 3, thus having a diminishing contribution to the relaxation time. This argument holds especially for smaller diameter cases.

IV. CONCLUSION

In conclusion, we did an extensive study of the mobility degradation mechanism due to the scattering between carriers and interfacial coupled phonon-plasmon mode in a 1-dimensional n-type Si nanowire under the presence of high- k gate dielectrics and polysilicon or metal gate electrode. We numerically calculated the mobility and observed its

increasing effect as the diameter becomes smaller. We also noticed a significant mitigating effect from metal gate. More complicated structures (such as the SiO₂ buffer layer) are planned for future study with the same framework.



Figs. 5, 6 and 7. Calculated channel electron mobilities due to scattering with interfacial soft phonons. Three body silicon radiuses are considered: (a) 3 nm, (b) 5 nm and (c) 9 nm. On each plot, we distinguish the poly gate cases (lines) and metal gate cases (symbols). For each family of symbols (lines) there are four cases of HfO₂ thickness correspondingly, ranging from 1.5 nm to 8 nm.

REFERENCES

- [1] G. Cohen et al, IEEE DRC, 187, 2008
- [2] M. Fischetti et al, J App Phys, Vol 89, 1232, 2001
- [3] M. Fischetti et al, J App Phys, Vol 90, 4587, 2001
- [4] Kotlyar et al, IEDM Tech. Dig. 391, 2004
- [5] L. Wendler et al, Phys. Rev. B. 49, 14531, 1994